VOL. 11, NO. 5, MARCH 2016 ISSN 1819-6608
ARPN Journal of Engineering and Applied Sciences

www.arpnjournals.com

COMPACT OPTICAL FILTER BASED ON MICRORING RESONATOR

N. Nadia Abd Aziz[1], Hazura Haroon[1] and Hanim Abdul Razak[2]
[1]Universiti Teknikal Malaysia Melaka, Hang Tuah Jaya, Durian Tunggal, Melaka, Malaysia
[2]Centre for Telecommunications Research Innovations (CETRI), Faculty of Electronic & Computer Engineering, Universiti Teknikal Malaysia Melaka, Hang Tuah Jaya, Durian Tunggal, Melaka, Malaysia
E-Mail: nurulnadia0@gmail.com

ABSTRACT

Optical filter that utilizes silicon micro-ring resonator (MRR) has been proposed as a solution in order to provide high-bandwidth, low power consumption and small size. MRR is the promising basic element of future optical integrated circuits due to its various applications such as wavelength filter, modulator and sensor. In this paper, we investigate the trade-off between ring radius, gap size and width of core variations to the MRR performance.

Keywords: silicon photonic, microring resonator, optical filter.

INTRODUCTION

Silicon photonics is becoming one of the important platforms that target the achievement of optical communications networks. One of the potential elements in silicon photonics integrated circuit design is microring resonator (MRR). Microring resonator has become an attractive multifunctional element for various optical communications applications in recent years, including optical modulator, sensor, multiplexing and wavelength filter [1]. This is due to its advantages of high Q-factor, compact size and less power consumption [2-3]. The capability of MRR to be fabricated on the silicon-on-insulator (SOI) exhibits a great potential in integration with CMOS electronics. Consequently, high index contrast devices can be harvested through lower fabrication cost.
Most of the recent research activities in optical field have been focusing on design and optimization of the MRR devices [4-5]. The important principles indicating a good performance of the MRR are wide free spectral range (FSR), high Q-factor, large extinction ratio and low insertion loss. The efficiency of the device is highly dependent on structure perfection resulting from the fabrication process.

Optical filter is one of the important devices that is used in wavelength-division-multiplexed (WDM) systems. It selects the desired wavelengths which pass the wanted channel and leave other channels uninterrupted. However, recent optical filters are too large. In WDM systems, a large bandwidth is important in order to provide a high information capacity. Therefore, optical filter based on MRRs is predicted to improve this necessity.

In this paper, our goal is to investigate the effect of design parameters variations on the MRR performance. Then, an appropriate architecture of optical filter was designed to achieve high FSR, high bandwidth, high Q-factor with lower loss and smaller size that is useful to the WDM systems.

THEORY

Silicon-on-insulator (SOI) waveguide should follow the expression for the single mode condition as mentioned by [6]:

$$w \times h \langle 0.13 \mu m^2 \quad (1)$$

where w and h are the width and height of the waveguide, respectively.

Figure-1 depicts an example of the mode profile simulation deploying SOI waveguide, which has a cross-section of 480 nm x 250 nm for TE polarized light by using Comsol Multiphysics 5.1. It can be clearly seen that due to high refractive index differences between silicon and silicon dioxide, strong confinement light can be observed at the centre of the rib waveguide.

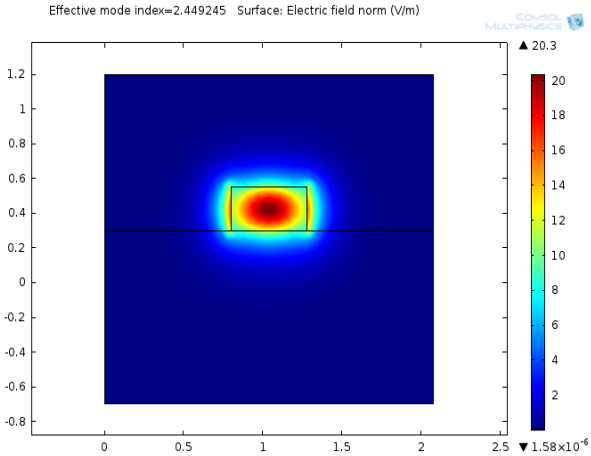

Figure-1. Mode profile SOI waveguide of 480 nm x 250 nm.

There are several numerical methods that can be utilized in microring resonator design and modeling. The most common is Finite Difference Time Domain (FDTD) by R-Soft, as well as SILVACO. In this paper, 3D electromagnetic simulator of CST Software is utilized [7]. The model is designed in 3D configuration.

Figure-2 shows the basic building block of MRR. The element consists of a ring waveguide coupled with the two straight waveguides, confined with the cladding.

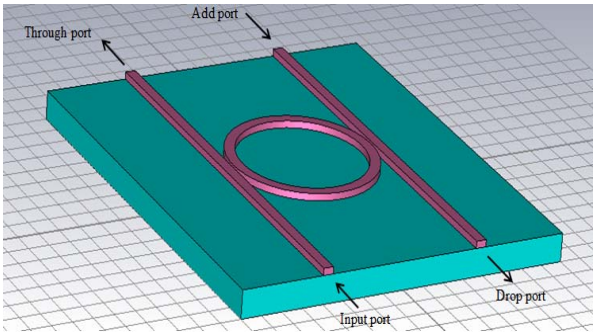

Figure-2. Basic building block of MRR.

Figure-3 shows the cross-section of the waveguide structure, which consists of two layers, silicon dioxide and silicon. The cladding is set as air. H is the height of the silicon dioxide, hw and hr is the height of the straight and ring waveguide, respectively. Meanwhile, ww is the width of the straight waveguide and wr is the width of ring waveguide. Ring radius and gap separation are denoted as R and g, respectively.

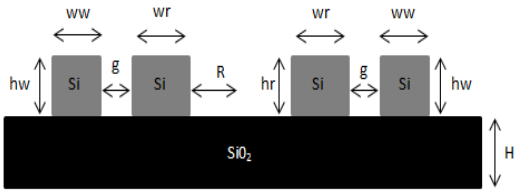

Figure-3. Cross-section of MRR.

This study focuses on the effect of varying ring radius, gap size between waveguide core and ring core, and also width of core to the overall performance of the MRR.

Theoretically, as the input light propagates from the laser beam into the input port and output port, the resulted signals can be observed from the through port and the drop port. When the input light is transmitted from input port and evanescently coupled to the ring, MRR is on resonance where the wavelength of the light fits a number of times inside the optical length of the ring [6].

$$\lambda_o = \frac{n_{eff} L}{m} \quad (2)$$

where m is an integer number.

The optical intensity in the ring is increased and higher than in the straight waveguide. This enhancement of intensity field can be measured by its finesse. The finesse is defined as in Eqn. (3) by [9]:

$$F = \frac{FSR}{FHWM} \quad (3)$$

Moreover, FSR can be calculated by the difference between two successive peaks of resonance and FWHM is the full width at half maximum of one peak. FSR can also be determined by Eqn. (4), [10]:

$$FSR = \frac{\lambda^2}{n_g L} \quad (4)$$

where ng is the group index and L is the physical path length, 2πR.

For the Q-factor of the resonance wavelength [11], mth is estimated by calculating the ratio of the operating wavelength to FWHM. It is important to measure the temporal confinement of light inside the ring resonator.

$$Q - factor = \frac{\lambda_o}{FWHM} \quad (5)$$

Meanwhile, extinction ratio is another performance characteristic that is defined as the ratio between output power and input power. It can be measured by observing the output power at the drop port and input power at the input port. In addition, insertion loss, IL is the ratio between the power received and the input power in decibel (dB) [12].

RESULTS AND DISCUSSIONS

In this work, TE-light was propagated in the waveguide in range of 1540-1580 nm and the output was scanned from this range. It is because the light is in low loss in this particular wavelength.

The refractive indexes for both substrates are 1.45 and 3.5, respectively. The core and cladding are set as silicon and silicon dioxide, respectively.

The design of MRR with R=6 µm, g=100 nm, h=250 nm and w=480 nm, the result was obtained and depicted as in Figure-4. The orange line shows the response observed from the through port, while the green line shows the response at the drop port. The MRR is on resonance at 1561.5 nm.

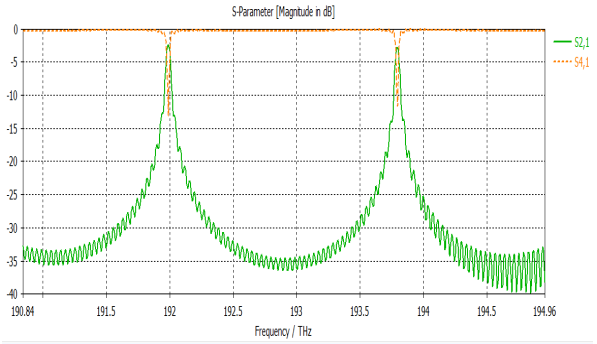

Figure-4. Through port and drop port transfer function of MRR.

With this basic design, the gap size, the width and the ring radius were varied in order to investigate the effect of the design dimension variations on the MRR performance.

In order to study the impact of gap size variations on MRR, three difference gap sizes were chosen, which are 100 nm, 150 nm and 200 nm [13]. The performance will be evaluated based on the insertion loss, extinction ratio, FSR and Q-factor.

The transmission spectrum observed at the drop port with varying gap size is presented in Figure-5. As the gap increased every 50 nm, the FSR was almost not affected. However, the calculated Q-factor was reduced. For example, for the gap size of 150 nm and 200 nm, Q-factor was 5219 and 3914, respectively. It shows that the gap size has significant effect on the MRR's performance. Meanwhile, the insertion loss increased as the gap size became smaller. For the gap size of 150 nm and 200 nm, the insertion loss was -0.31 dB and -0.27 dB, respectively.

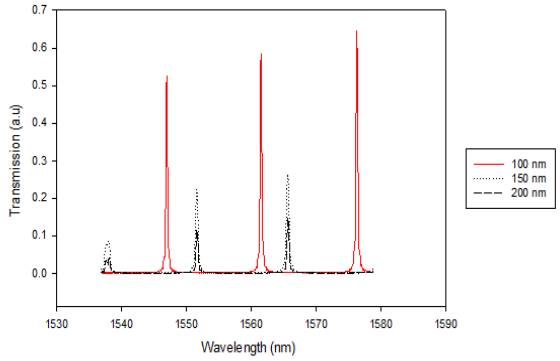

Figure-5. Transmission response of MRR with various gap sizes.

The size of the core width is also crucial in order to acquire the optimum design. To investigate the effect of core width on the performance of MRR, the core width value was varied from 480 nm to 450 nm and 420 nm. The output results are portrayed in Figure-6.

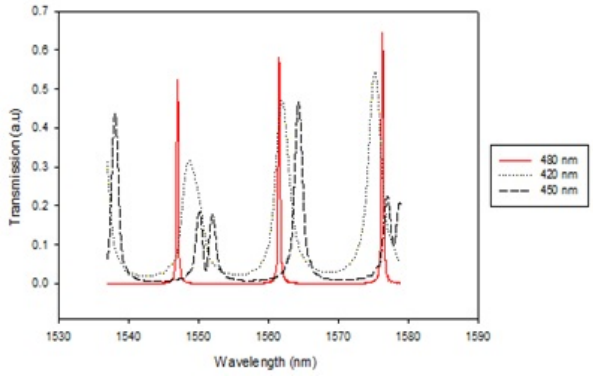

Figure-6. Transmission response of MRR with width of core.

It is noticeable that the FSR is almost constant. However, the Q-factor computed slightly reduced as the width shrunk. For instance, for the width of 450 nm and 420 nm, the values of Q-factor were 5219 and 3914, respectively. In contrast, the insertion loss was reduced as the width became larger. In addition, it can be observed that the extinction ratio was getting smaller as the width was reduced.

The other crucial parameter in designing the MRR is radius of the ring. The three ring radii chosen were 3 µm, 6 µm and 9 µm. The result is depicted in Figure-7. It is obvious that from Figure-7, smaller ring radii produce larger Q-factor and FSR. Based on Table-1, for example, the FSR and Q-factor of R=3 µm is 28 nm and 7807, respectively compared to the R=6 µm is 14.5 nm and 5219. The result agrees well with the theory which stated that FSR is inversely proportional to the ring diameter [14]. It is also obvious that ring radius has less effect on insertion loss.

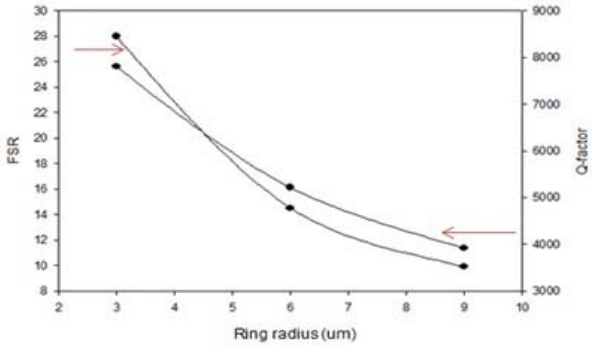

Figure-7. Q-factor and FSR of the varying ring radius.

Table-1. Results of various ring radii for MRR.

Radius, nm	3	6	9
λ_o	1566.0	1561.5	1563.0
FSR[nm]	28.0	14.5	9.9
Q-factor	7808	5219	3914
Insertion Loss (dB)	-0.13	-0.12	-0.12
Extinction Ratio (dB)	45.5	10.7	7.4

CONCLUSIONS

From the simulation, it can be concluded that it is important to choose the suitable parameters in order to produce the appropriate design of MRR. It proves that these parameters have an effect on MRR performance principle that compact size of the device can provide higher FSR and Q-factor. The obtained results will be a useful guidance for upcoming laboratory works.

ACKNOWLEDGEMENTS

The authors would like to thank University Teknikal Malaysia Melaka (UTeM) for the support. This research work is supported by funding from UTeM (PJP/2013/FKEKK(43C)/S01260.

REFERENCES

[1] Alan R. Mickelson. 2011. Silicon photonics for on-chip interconnections. IEEE Custom Integrated Circuits Conf.

[2] Moustafa Mohamed, Zheng Li, Xi Chen, Alan Mickelson, Li Shang. 2011. Modeling and Analysis of Micro-Ring Based Silicon Photonic Interconnect for Embedded Systems. CODES+ISSS'11. 227-236.

[3] Hazura Haroon, Sahbudin Shaari, PS Menon, Hanim Abdul Razak, Mardiana Bidin. 2013. Application of Statistical Method to Investigate the Effects of Design Parameters on the Performance of Microring Resonator Channel Dropping Filter. International Journal of Numerical Modelling: Electronic Networks, Devices and Fields. 26 (6): 670-679.

[4] H. Hazura, A. R. Hanim, B. Mardiana, Sahbudin Shaari & P. S. Menon. 2011. Free Carrier Absoption Loss of p-i-n Silicon-On-Insulator (SOI) Phase Modulator. AIP Conf. Proc. 241.

[5] Q. Xu, D. Fattal, R. G. Beausoleil. 2008. Silicon Microring Resonators with 1.5-um Radius. Opt. Express 16. 4309-4315.

[6] Grahan T. Reed. 2008. Silicon Photonics the State of The Art (John Wiley & sons, Ltd).

[7] Riyadh D. Mansoor, Hugh Sasse, Mohammed Al Asadi, Stephen J. Ison, Alistair P. Duffy. 2014. Over Coupled Ring Resonator-Based Add/Drop Filters, IEEE Journal of Quantum Electronics. 50: 598-603.

[8] 3D Electromagnetics Simulation software. http:// www.cst.com.

[9] Sasan Fathpour, Bahram Jalali. 2012. Silicon Photonics for Telecommunications and Biomedicine (Taylor & Francis Group).

[10] B. Mulyanti, P.S Menon, S. Shaari, T. Hariyadi, L. Hasanah, H. Haroon. 2014. Design and Optimization of Coupled Microring Resonators (MRRs) in Silicon-On-Insulator. Sains Malaysian. 43(2): 247-252.

[11] Fakhrurrozi, S. A. Santoso, Octarina Nur S, Ary Syahriar. 2013. Temperature Effects on Parallel Cascaded Silica Based Microring Resonator. International Conference of Information and Communication Technology (ICoICT). 367-371.

[12] El-hang Lee, Louay A. Eldada, Manijeh Razeghi, Chennupati Jagadish. 2011. VLSI MICRO-and NANOPHOTONICS Science, Technology, and Applications (Taylor & Francis Group).

[13] Preecha P. Yupapin, Chat Teeka, Muhammad Arif Jalil, Jalil Ali. 2012. Nanocsale Nonlinear PANDA Ring Resonator (Taylor & Francis Group).

[14] H. Hazura, M. Bidin, HA Razak, PS Menon, N Arsad, ZFM Napiah. 2011. Impact of Coupled Resonator Geometry on Silicon-On-Insulator Wavelength Filter Characteristics. IEEE Regional Symposium on Micro and Nanoelectronics (RSM). 380-382.